

# Free surface instability of non-Newtonian laminar flows

## Les instabilités de surface libre des écoulements laminaires non Newtoniens

ZHAO-YIN WANG, *Prof. Dept. of Hydraulic Engineering, Tsinghua University, Beijing 100084, China, Vice Secretary General of International Research and Training Center on Erosion and Sedimentation, email: zywang@tsinghua.edu.cn*

### ABSTRACT

The mechanism of free surface instability of non-Newtonian laminar flows is studied theoretically and experimentally in the paper. Development of surface waves and roll waves of non-Newtonian flow has been reported in many cases, such as the river clogging in the hyperconcentrated flows, intermittent viscous debris flows and fluctuation in mudflows. Theoretical analysis from the equation of motion incorporating the non-Newtonian nature of the fluid demonstrated that the free surface instability is essentially caused by the yield stress. Two dimensionless numbers,  $S_y$  and  $S_{vis}$ , representing the effects of yield stress and viscosity are calculated and compared for various flows. It is concluded that the free surface is unstable and roll waves may develop even at constant incoming flow rate if  $S_y$  is much larger than  $S_{vis}$  and is stable if  $S_y$  is smaller than  $S_{vis}$ . Experiments were conducted to study the phenomena of river clogging, development of a perturbation wave in non-Newtonian laminar flow, and development of roll waves. The results agree well with the theoretical formula showing exponential law of growth of wave height. The growth rate of wave height depends essentially on the parameter  $S_y$ . If  $S_y$  is large enough a series of roll waves develop from stable flow and the larger is the parameter, the higher the waves.

### RÉSUMÉ

Le mécanisme des instabilités de surface libre des écoulements laminaires non newtoniens est étudié dans cet article en théorie et expérimentalement. Le développement de ondes et de roll waves à la surface d'écoulements non newtoniens a été mentionné dans de nombreux cas tels que l'engorgement des rivières par des écoulements hyper concentrés, les écoulements intermittents de déblais visqueux, et les fluctuations dans les coulées boueuses. L'analyse théorique, à partir des équations du mouvement, en tenant compte de la nature non newtonienne du fluide, montre que l'instabilité de la surface libre est essentiellement due à la contrainte d'écoulement (modèle de Bingham). Deux nombres sans dimension,  $S_y$  et  $S_{vis}$ , représentant les effets de la contrainte et de la viscosité, sont calculés et comparés pour divers écoulements. On en conclut que la surface libre est instable et peut développer des roll waves même à débit d'amont constant si  $S_y$  est beaucoup plus grand que  $S_{vis}$ , et qu'elle est stable si  $S_y$  est inférieur à  $S_{vis}$ . Les expériences ont été faites pour étudier l'engorgement des rivières, le développement d'une onde de perturbation dans un écoulement laminaire non newtonien, et le développement de roll waves. Les résultats sont en bon accord avec la formule théorique donnant la loi exponentielle de croissance de la hauteur de vague. Le taux de croissance de la hauteur de vague dépend essentiellement du paramètre  $S_y$ . Si  $S_y$  est assez grand, une série roll waves se développe à partir de l'écoulement stable, et, plus ce paramètre est grand, plus les vagues sont hautes.

**Key words:** Free surface instability. Non-Newtonian flow, Roll waves, River clogging, Yield stress.

## 1 Introduction

Transitions of an open channel flow from one type to another occurs as a result of instability of the former, which is related to a special property of the fluid, e.g. turbulence generates from instability of laminar flow due to high viscous shear. Tritton (1977) gave a description of the surface tension instability of a liquid column. The basic state is a cylindrical column of liquid, such as tape water flowing from a cock, which is held together by the action of surface tension. Such a column may develop corrugations in its shape and ultimately breaks into discrete drops because the pressure gradient generated by a small perturbation in surface shape pushes fluid in directions that amplify the original perturbation. Newtonian open channel flow may develop into roll waves (Vedernikov, 1946). Chen discussed the stability criterion of Newtonian open channel flow and indicated that the Vedernikov number can be used as the criterion and evaluated the role of velocity distribution in the free surface stability (Chen, 1995)

Similarly instability of non-Newtonian fluid flow may occur due to its rheological properties as a random perturbation is presented. The most important non-Newtonian fluid is clay and silt suspension which occurs frequently in nature. The most simple constitu-

tion equation of a non-Newtonian fluid is given by the Bingham model

$$\tau = \tau_B + \eta \varepsilon \quad (1)$$

in which  $\tau$  is the shear stress of the flow,  $\tau_B$  the yield shear stress of the fluid,  $\eta$  the rigidity coefficient (called as Bingham viscosity by some researchers) and  $\varepsilon$  the shear rate which is equal to the velocity gradient in laminar flow. Bingham fluid can flow in an open channel only as the maximum driving shear stress is larger than the yield shear stress, or the flow depth  $h$  is larger than a critical depth

$$h_c = \frac{\tau_B}{g \rho_m J} = \frac{\tau_B}{\gamma_m J} \quad (2)$$

in which  $J$  is the energy slope,  $g$  the gravity acceleration,  $\rho_m$  the density and  $\gamma_m$  the specific weight of the fluid (especially clay and silt suspension).

Engelund and Wan (1984) conducted an experiment with non-Newtonian clay suspension. They used a 71 cm-long closed conduit with cross section 3.48 cm wide x 1 cm high connecting a

Revision received July 14, 2000. Open for discussion till December 31, 2002.



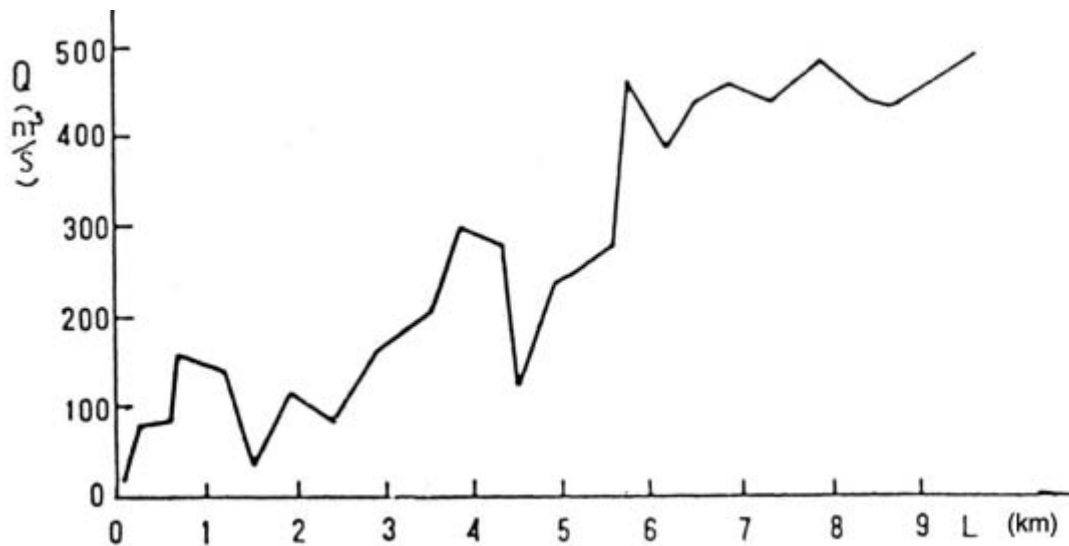


Fig. 2. Variation of discharge along the course of a debris flow in the Little Almarkingka River on August 7, 1956.

Water-stone debris flow also exhibit intermittence, e.g. the stone debris flows triggered by rainstorms at Mount Unzen and Mount Merapi, Japan, appear as a series of surges. The source material consists of clasts of decite lava. (Suwa et al., 1996). It is remarkable that the time interval of the surges in the mid stage of the events is almost constant, which is nearly one minute. The mechanism of the instability is different from those of the viscous debris flow because the matrix is Newtonian.

Life span of reservoirs depends mainly on the rate of sedimentation. In order to release sediment from the Hengshan Reservoir in Shanxi, China and extend its useful life, the managers often empty the reservoir and allow the incoming water to erode the

deposit. The outflow is hyperconcentrated and often develops into a fluctuating or intermittent flow because of the non-Newtonian nature (Guo et al., 1985). The author conducted a model experiment to simulate scouring cohesive sediment from an emptied reservoir and observed the same phenomenon. Fig. 3. shows the discharge and sediment concentration of mudflow sluiced out of the reservoir, in which  $S$  is the sediment concentration in weight of sediment per volume (Wang, 1992). The mudflow was very unstable because of its large yield stress. Sometimes the discharge of the mudflow reduced to zero and the flow became intermittent. The intermittent nature also occurred in mudflows at Wrightwood, USA. Mudflows in the upper part of Health Creek consisted of flows with blunt, rocky snouts. Downstream, transitory waves were generated within a moving flow and had a velocity about twice that of the flow. Similar waves were also observed in the 1941 mudflows and 1972 mudflows (Morton and Campbell, 1974).

There are still quite a lot of ambiguities concerning the instability of the non-Newtonian flow. Much more definite mechanism for the instability of non-Newtonian flow and intermittent surges of debris flow are left to be studied intensively. The author conducted experimental and theoretical studies on the mechanism and indicated that the instability is attributed to the yield stress of the fluid (Wang et al., 1990). This study is a continuation of the mechanism study with further more experimental results and further development and application of the theory.

## 2. Mechanism of the instability.

For unsteady open channel flow, the one-dimensional continuity equation and equation of motion are

$$\frac{\partial h}{\partial t} + u \frac{\partial h}{\partial x} + h \frac{\partial u}{\partial x} = 0 \quad (3)$$

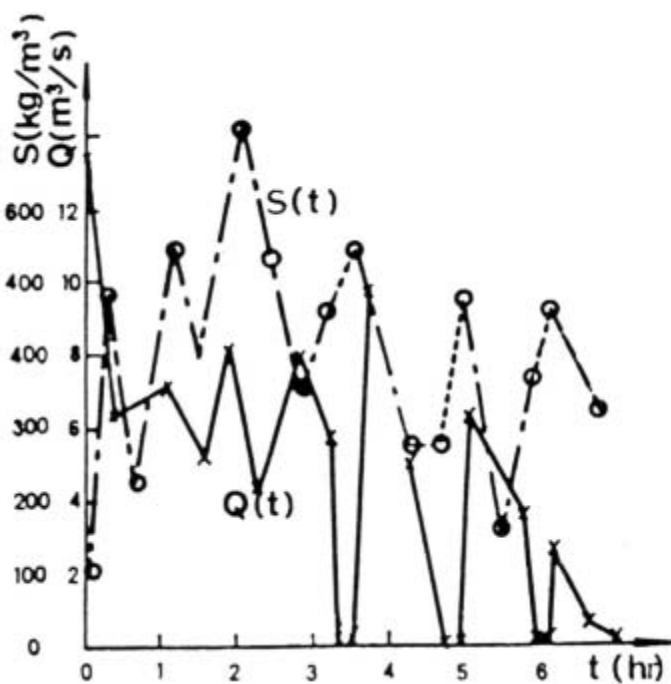


Fig. 3. Instability of discharge and sediment concentration of mud flow in a model test to simulate scouring cohesive sediment from a reservoir

$$\frac{\partial u}{\partial t} + u \frac{\partial u}{\partial x} + g \frac{\partial h}{\partial x} = gJ - \frac{\tau_0}{\rho_m h} \quad (4)$$

where  $u$  is the average velocity,  $\tau_0$  is the shear stress of the flow acting on the bed, or the resistance of the bed to the flow. With the method of the characteristics, the two partial differential equations can change into two groups of normal differential equations in which one group follows the  $C_1$ -family of characteristic curves

$$\frac{dx}{dt} = u + \sqrt{gh} \quad (5)$$

$$\frac{d}{dt}(u + 2\sqrt{gh}) = gJ - \frac{\tau_0}{\rho_m h} \quad (6)$$

and another group follows the  $C_2$ -family of characteristic curves

$$\frac{dx}{dt} = u - \sqrt{gh} \quad (7)$$

$$\frac{d}{dt}(u - 2\sqrt{gh}) = gJ - \frac{\tau_0}{\rho_m h} \quad (8)$$

In steady uniform flow, the velocity  $u$  and the depth  $h$  are constants, and the frictional resistance must then be equal to the tractive force, i.e.

$$gJ = \frac{\tau_0}{\rho_m h} \quad (9)$$

If a perturbation induces increments  $\Delta u$ ,  $\Delta(2\sqrt{gh})$  and  $\Delta(\tau_0/\rho_m h)$ , Then Eq.(6) becomes

$$\begin{aligned} \frac{d}{dt}(u + 2\sqrt{gh} + \Delta u + \Delta(2\sqrt{gh})) \\ = gJ - \frac{\tau_0}{\rho_m h} - \Delta\left(\frac{\tau_0}{\rho_m h}\right) \end{aligned} \quad (10)$$

If one subtracts Eq.(6) from Eq.(10), the result is

$$\frac{d}{dt}(\Delta u + \Delta(2\sqrt{gh})) = -\Delta\left(\frac{\tau_0}{\rho_m h}\right) \quad (11)$$

Eq.(11) is called a perturbation equation along the  $C_1$ -family of characteristic curves. Similarly, the perturbation equation along the  $C_2$ -family of characteristic curves is

$$\frac{d}{dt}(\Delta u - \Delta(2\sqrt{gh})) = -\Delta\left(\frac{\tau_0}{\rho_m h}\right) \quad (12)$$

In a steady laminar flow of a Bingham fluid, the shear stress  $\tau_0$  equals  $\tau$  given by Eq.(1). Fig. 1. shows the general velocity distribution of Bingham flow in an open channel. The upper part is a flow plug in which the fluid flows at a uniform velocity  $u_p$ , which nearly equal to the average velocity  $u$ . Only in the zone near the bed does the velocity vary, from zero to  $u_p$ . The thickness of the

layer is assumed  $d$ . The velocity gradient, therefore, is roughly  $u/d$ , and

$$\frac{d}{dt}(\Delta u + \Delta(2\sqrt{gh})) = -\Delta\left(\frac{\tau_B}{\rho_m h} + \eta \frac{u}{\rho_m h d}\right) \quad (13)$$

As shown in Fig. 4., a perturbation that occurs at point  $A(x,t)$  in the  $x-t$  plane will propagate along the characteristic curves. For any point  $B$  on the  $C_1^1$  characteristic curve that passes through the point  $A(x,t)$ , a characteristic curve  $C_2^2$  intersects the  $C_1^1$  curve at point  $B$ . The dotted area is undisturbed. The initial perturbation has no effect on the area, and the velocity  $u$  and depth  $h$  in it remain constant. Integration of Eq.(12) along the  $C_2^2$  characteristic curve yields

$$\Delta u - \Delta(2\sqrt{gh}) = \int_{B'}^B -\Delta\left(\frac{\tau_0}{\rho_m h}\right) dt \quad (14)$$

Point  $P$  is always in the undisturbed area as it moves from  $B'$  to a point near  $B$ , and  $\Delta(\tau_0/\rho_m h)$  is zero in the process of integration except at the point  $B$ . Since  $\Delta(\tau_0/\rho_m h)$  is not infinite at  $B$ , Eq.(14) gives

$$\begin{aligned} \Delta u - \Delta(2\sqrt{gh}) &= 0 \\ \text{or} \\ \Delta u &= \Delta(2\sqrt{gh}) \end{aligned} \quad (15)$$

For a low discharge of mudflow, the average velocity is small. If the yield stress of the mud is large, the second term on the right hand side of Eq. (13) is negligible, and Eq.(13) can be rewritten as

$$\frac{d}{dt}\left(\sqrt{\frac{g}{h}}\Delta h\right) = -\frac{1}{2}\Delta\left(\frac{\tau_B}{\rho_m h}\right) = \frac{1}{2}\frac{\tau_B}{\rho_m h^2}\Delta h \quad (16)$$

In the process, Eq.(15) and the following formulas

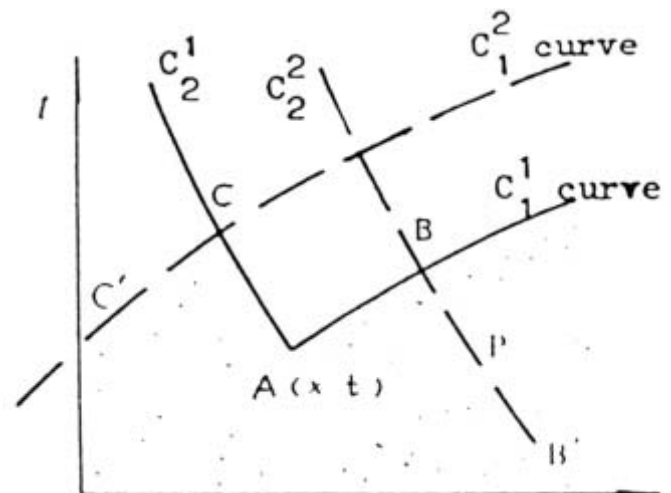


Fig. 4. Characteristic curves on  $x-t$  plane.

$$\Delta(2\sqrt{(gh)}) = \frac{d}{dh}(2\sqrt{(gh)})\Delta h = \sqrt{(g/h)}\Delta h \quad (17)$$

$$\Delta\left(\frac{\tau_B}{\rho_m h}\right) = \frac{d}{dh}\left(\frac{\tau_B}{\rho_m h}\right)\Delta h = -\frac{\tau_B}{\rho_m h^2}\Delta h \quad (18)$$

have been used.

The integration of Eq.(16) yields

$$\frac{\Delta h}{\Delta h_0} = e^{\frac{\tau_B}{2\sqrt{(gh)}\rho_m h}t} \quad (19)$$

where  $\Delta h_0$  is the initial perturbation in depth.

Eq.(19) indicates that the initial perturbation  $\Delta h_0$  will grow, and the larger the yield stress  $\tau_B$  and the smaller the mud depth  $h$ , the faster the wave will grow. After a perturbation develops into a roll wave, the continuities of velocity and depth no longer hold, thence Eq.(19) does not hold true. Therefore, the wave height can not grow up indefinitely.

If the average velocity  $u$  and the rigidity coefficient  $\eta$  are large and the yield stress is small, the second term on the right hand side of Eq. (13) is much larger than the first one, and Eq.(13) may be rewritten as

$$\frac{d}{dt}(\Delta u) = -\frac{1}{2}\Delta\left(\frac{\eta u}{\rho_m h d}\right) \quad (20)$$

in which Eq.(18) has been employed. Since

$$\begin{aligned} \Delta\left(\frac{\eta u}{\rho_m h d}\right) &= \frac{\partial}{\partial u}\left[\frac{\eta u}{\rho_m h d}\right]\Delta u + \frac{\partial}{\partial h}\left[\frac{\eta u}{\rho_m h d}\right]\Delta h \\ &= \frac{\eta u}{\rho_m h d}\left(\frac{\Delta u}{u} - \frac{\Delta h}{h}\right) = \frac{\eta}{\rho_m h d}(1 - Fr)\Delta u \end{aligned} \quad (21)$$

Eq.(20) can be rewritten as

$$\frac{d}{dt}(\Delta u) = -\frac{\eta}{2\rho_m h d}(1 - Fr)\Delta u \quad (22)$$

or after integration

$$\frac{\Delta u}{\Delta u_0} = e^{-\frac{\eta(1-Fr)}{2\rho_m h d}t} \quad (23)$$

where  $\Delta u_0$  is the initial perturbation in velocity,  $Fr = u/\sqrt{(gh)}$  is the Froude number.

Eq.(23) proves that in high flow velocity of high yield stress and small yield stress, as long as  $Fr < 1$ , the perturbation in velocity  $\Delta u_0$  always decreases, hence, the flow is stable.

Eqs. (19) and (23) give the results for the two extreme cases. In the general case, both terms on the right hand side of Eq.(13) should be taken into account. Then

$$\frac{d}{dt}(\Delta u) = \frac{1}{2\rho_m h}\left[\frac{\tau_B}{\sqrt{(gh)}} - \frac{\eta}{d}(1 - Fr)\right]\Delta u \quad (24)$$

If the fluid has a large yield stress and the Froude number is larger than one, the flow will be very unstable and develops into roll waves quickly. Many viscous debris flows in the Jiangjia Ravine are examples of such flows (Kang, 1985). If the Froude number is smaller than one but the rigidity coefficient  $\eta$  is small and the yield stress large, the flow is also unstable and develops into wave flow. Some unstable hyperconcentrated flows in the tributaries of the Yellow River are examples of such type of flow. Whereas if the yield stress is small and  $\eta$  is large, a non-Newtonian flow is stable at low Froude number, e.g. flows of crude oil and lava are stable because magma is of extremely high rigidity coefficient.

The two terms on the right hand side of Eq.(13) are normalised with the gravity acceleration  $g$ :

$$S_y = \frac{\tau_B}{g\rho_m h} \quad (25)$$

$$S_{vis} = \frac{\eta u}{g\rho_m h d} \quad (26)$$

represent the importance of the yield shear stress and the rigidity of the clay suspension. If  $S_y$  is much larger than  $S_{vis}$ , any perturbation will grow up and the flow is in unstable state, and if  $S_{vis}$  is larger than  $S_y$  and the Froude number is smaller than 1 the non-Newtonian laminar flow is stable.

The foregoing discussion is based on the perturbation equation along the C1-family of characteristic curves. For perturbation at point A(x,t) propagating along the C2-family of characteristic curves, similar discussion yields that no matter how large the discharge and the depth are, the  $\tau_B$ -term or  $\eta$ -term dominates the resistance; hence the perturbation always declines. In other words, the wave does not move upstreamward in any cases.

One can reason that if the fluid is a pseudo-plastic fluid with the constitutional equation:

$$\tau = K\varepsilon^{1/m}, \quad m > 1 \quad (27)$$

the flow in open channel can also be unstable. The function of coefficient  $K$  is similar to  $\eta$  and  $m$  similar to  $\tau_B$  with regard to the instability of non-Newtonian fluid flow.

### 3. Experimental study

#### 3.1 Experimental Conditions

The experiments were conducted in a 26-m long, 0.6-m wide and 0.5-m high tilting flume with glass sided walls. The original channel bed was made of steel plate and was hydraulically smooth even for flow of water and the bed slope can be adjusted in the range 0-0.05. Clay suspensions were recirculated through the channel. The flow rate was controlled by means of an inlet valve

and measured by using a magnetic flowmeter. For supercritical flow of Froude number larger than one, the tailgate was open allowing flow out off freely. For subcritical flow, the flow depths were adjusted by means of an overflow weir at the downstream end of the channel to achieve uniform flow conditions. The water depth was measured by using scaling arrow with digital readout to within 0.1 mm at worst. Except for a few experiment the depth of the flow was in a range from 1 to 12 cm, which yielded width to depth ratios larger than 5:1, so that the flow was effectively two dimensional and free from wall effects in the central zone of the channel.

The clay material has a density of 2.68 g/cm<sup>3</sup> and median diameter of 0.002 mm. The main mineral compositions were montmorillonite, quartz, illite and calcite. Clay and tap water was well mixed and the suspensions behaved like a viscous liquid rather than solid water mixture. Clay concentrations of the samples were analysed by using picnometer. The measurement error of concentration was 0.0004. The pH value of the suspensions was 7.2. The rheologic behavior of the suspensions was studied with a rotating coaxial cylinder viscometer (Wang, Larsen and Xiang, 1994). Samples of clay suspensions were taken from the flume and tested with the viscometer. For concentrations of less than 1.6%, the suspension exhibits very small yield stress and can be regarded still Newtonian but with high viscosity. For higher concentrations, it showed obvious yield stress and roughly followed the Bingham rheological model given by Eq.(1). The temperature of water and clay suspensions was maintained in the range 19-22°C for all experiments. The effect of the variation in temperature on the rheological properties was negligible. The yield stress and rigidity coefficient increase with clay concentration and follow the empirical formulas:

$$\tau_B = \tau_{Bm} C_v^{3.7} \quad (28)$$

$$\eta = \mu (1 - 3.6 C_v)^{-2.5} \quad (29)$$

in which  $\tau_{Bm} = 12000$  Pa and  $\mu$  is the viscosity of clear water,  $C_v$  is the volume concentration of clay.

A video camera and a sounding meter were used to record the development of the waves. The velocity was measured by using a one component pressure velocimeter. The tip of the sensor is 1 mm in diameter. The probe size, working principle, calibration and relative error of measurement are presented in a literature (Wang et al., 1995). The velocimeter can measure turbulence with sampling frequency 300 Hz. All the flows were laminar because the clay suspensions were high viscous.

### 3.2 Channel Clogging

The phenomenon of river clogging was investigated in the experiment with clay suspensions of 5 different concentrations and 3 bed slopes. For given bed slopes and clay concentrations the overflow weir was adjusted for different flow discharges to achieve uniform and stable flows. Then the discharge and the overflow weir were slowly reduced until river clogging occurred. The clay suspension with a thickness up to 30 cm stopped moving because

the driving shear stress was balanced by the yield shear stress of the suspension. After a while the suspension suddenly flowed again, like a wave propagating down the flume, because the continuous incoming discharge rose the surface slope and driving shear stress. After the wave passed the suspension came to standstill again until second wave occurred. Table 1 presents the critical conditions under which the phenomenon of river clogging occurred, in which  $\tau_0$  is the driving shear stress, T the period of the clogging. Only as the shear stress was smaller than or close to the yield stress of the suspension, river clogging occurred, which demonstrates the yield stress is the essential reason for the river clogging. Measurement of the velocity in a few experiments indicates that the flows were laminar. The probe showed fluctuation of velocity when a wave passed, which is much different from turbulence in its frequency 100 times lower than that of normal turbulence. Over most upper part of the flow there was no velocity gradient. The zone is called plug. There was a thin layer close to the bed, in which velocity gradient exists. The thickness of the layer, d, and the velocity gradient in the layer were unstable, which caused the velocity of the plug zone fluctuating as shown in Fig. 5. Roll waves occurred if the flow depth was small. It differs from the river clogging in its small period and nearly zero depth of clay suspension between the waves. There was almost no or very limited still suspension after a wave passed.

Table 1. Critical conditions for river clogging

No.	J (%)	Q(l/s)	h(m)	$C_v$ (%)	$\eta$ (Poise)	$\tau_B$ (Pa)	$\tau_0$ (Pa)	T(min.)	Note
1	0.4	4	0.02	5.1	0.0166	0.264	-	-	No clogging
2	0.4	7	0.04	8.5	0.0249	1.75	1.8	30	River clogging
3	0.8	3.4	0.017	8.5	0.0249	1.75	1.5	23	Roll waves
4	1.2	4	0.012	8.5	0.0249	1.75	1.61	6	Roll waves
5	0.4	8	0.07	11.3	0.0369	5.02	4.9	41	River clogging
6	0.8	6	0.05	11.3	0.0369	5.02	4.7	26	and measure u
7	1.2	5	0.035	11.3	0.0369	5.02	4.9	23	River clogging
8	0.4	12	0.30	15.8	0.0819	17.34	14.8	33	River clogging
9	0.8	10	0.16	15.8	0.0819	17.34	15.8	28	River clogging
10	1.2	9	0.11	15.8	0.0819	17.34	16.2	22	and measure u
11	0.8	13	0.29	19.0	0.178	34.3	29.8	26	River clogging
12	1.2	10	0.18	19.0	0.178	34.3	27.8	23	River clogging

### 3.3 Instability Induced by Perturbation

Experiments were conducted to study the growth of perturbation in non-Newtonian laminar flow and validate the theory proposed in the above chapter. Table 2 presents the flow conditions and the main results of the experiments. The yield stress and the rigidity coefficient of the clay suspensions can be found in Table 1 of the same concentrations. Measurement showed that all the flows were laminar and the upper part of the flows, of about 80% of the depth, was a plug and flowed at a uniform velocity. The plug velocity  $u_p$  was measured by the velocimeter and is presented in the Table 2, which is slightly larger than the average velocity. The dimensionless yield stress and viscosity parameter,  $S_y$  and  $S_{vis}$ , are also presented in the table. For flows of low concentration at high

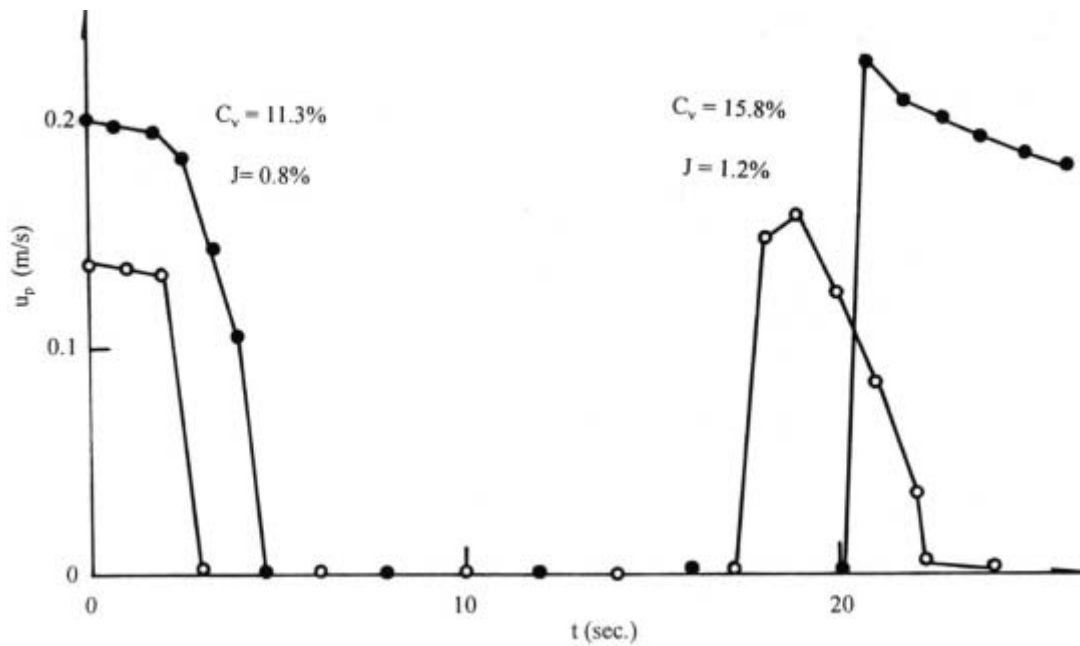


Fig. 5. Plug velocity of clay suspensions varying during the river clogging.  
 (•  $C_v=11.3\%$ ,  $J=0.8\%$  and  $T=26$  s; ×  $C_v=15.8\%$ ,  $J=1.2\%$  and  $T=22$  s)

discharge  $S_{vis}$  was in the same order or even larger than  $S_y$ , any perturbation did not grow up obviously and the results are not presented in the table. In fact, if  $h_o$  given by Eq. (2) is small (low concentration and low yield stress) and the flow depth is large (high discharge), or the flow depth is much larger than  $h_o$ , the flow is stable. For flows of high concentration at low discharge  $S_y$  was much larger than  $S_{vis}$ , as shown in Table 2, therefore, the flows were dominated by the yield stress. The flow was in unstable state and perturbation could grow up into big waves and the solution Eq.(19) is applicable.

Table 2 Experimental results of the induced instability

No.	$C_v$ (%)	$J$ (%)	$Q$ (l/s)	$h$ (m)	$u_p$ (m/s)	$Fr$	$S_y$	$S_{vis}$	$\tau_B/2\gamma_m h$	$\Delta h/L$
13	19	2.0	25	0.14	0.31	0.254	0.019	0.0006	0.009	0.007
14	19	3.0	20	0.095	0.38	0.363	0.028	0.0009	0.014	0.008
15	19	4.0	27	0.074	0.67	0.714	0.036	0.0016	0.018	0.009
16	15.8	4.0	12	0.04	0.58	0.798	0.035	0.0021	0.017	0.009
17	15.8	3.0	37	0.055	1.19	1.526	0.026	0.0022	0.013	0.004
18	15.8	2.0	50	0.08	1.12	1.170	0.018	0.0011	0.0087	0.004
19	15.8	1.2	35	0.125	0.50	0.421	0.011	0.0004	0.0056	0.004
20	11.3	1.2	32	0.045	1.33	1.784	0.009	0.0011	0.0048	0.002
21	11.3	0.8	13	0.06	0.40	0.470	0.007	0.0004	0.0036	0.002
22	11.3	0.4	50	0.11	0.80	0.729	0.004	0.0003	0.002	0.001
23	8.5	0.4	28	0.05	0.95	1.332	0.003	0.0004	0.0016	0.001
24	8.5	0.8	28	0.03	1.71	2.860	0.005	0.0012	0.0027	0.001

Under the flow conditions in Table 2 the flow was stable if no perturbation were introduced. The perturbation was presented by feeding 3-5 litres of extra clay suspension from a feeding tank into the flow at 2 m from the entrance. Initially the feeding caused very limited surface wave but it grew up down the flume. From Eq.(15) we have

$$\Delta u = \Delta(2\sqrt{gh}) = \sqrt{\frac{g}{h}}\Delta h \quad (30)$$

The distance for a wave to travel in time  $t$  is

$$L = \int_0^t (u_p + \Delta u) dt \quad (31)$$

Employing eq.(19) and (30) we obtain

$$L = u_p t + \frac{2\gamma_m h}{\tau_B} \Delta h_0 e^{\frac{\tau_B t}{2\rho_m \sqrt{ghh}}} \quad (32)$$

If  $u_p$  is small compare with propagation speed of the perturbation wave  $\Delta u$ , the growth rate of the perturbation wave height per distance is given as follows:

$$\frac{\Delta h}{L} = \frac{\tau_B}{2\gamma_m h} = \frac{1}{2} S_y \quad (33)$$

The equation explains that the larger the yield stress and the smaller the flow depth the higher the growth rate of the perturbation wave propagating down the stream. Table 2 shows the measured growth rate  $\Delta h/L$  and the value of  $\tau_B/2\gamma_m h$ . The former is smaller than the latter because the magnitude of the flow velocity is in the same order as that of the propagation speed. Roughly the measured growth rate is about half of those given by Eq.(33), as given in Fig. 6.

Fig. 7. shows the growth curve of the perturbation wave height. The curves follows the exponential law as given by Eq.(19) in the development part but tends to constant after it grew to a certain value of  $\Delta h$ . The larger the yield stress, the closer the depth to the critical depth  $h_o$ , the faster the wave grows up. The discharge at

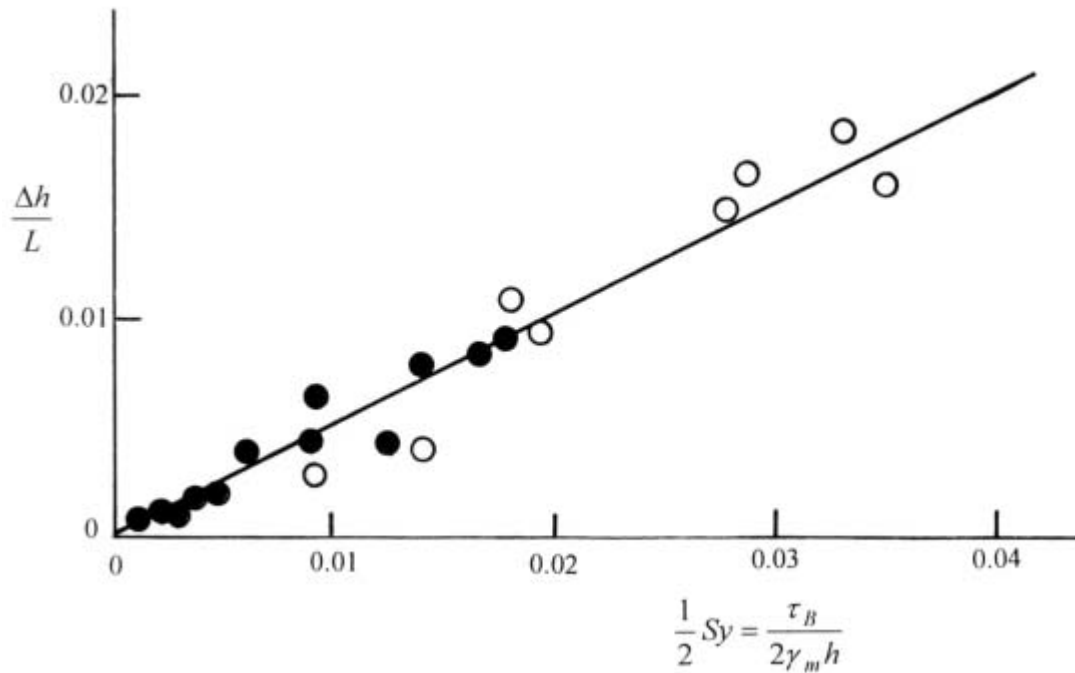


Fig. 6. Growth rate per distance of the wave height  $\Delta h/L$  as a function of the dimensionless parameter  $\tau_B/\gamma_m h$ .

2 meters from the entrance and the tailgate (26 m from the entrance) are shown in Fig. 8a. The discharge at the tailgate was estimated from the depth of the flow over the tailgate weir recorded by the video camera. In the figure  $Q$  is the constant discharge into the flume,  $Q_0$  is the perturbation discharge fed into the flow,  $Q_{out}$  is the measured discharge at the tail gate and  $V_{out}/V_0$  is the ratio of the wave volume at the tail gate and the perturbation. The highest discharge and the volume of the wave at the tailgate were 5-15 times of the initial perturbation wave. The

same phenomenon was also measured in an earlier experiment in a flume 8.7 m long and 10 cm wide by the author (Wang et al., 1990), as shown in Fig. 8b. Clay concentrations  $C_v=0.19$  for No.15,  $C_v=0.14$  for No.26, 28, 31 were used in the experiment. The horizontal dashed lines represent the stable base flow,  $Q_0$  and  $Q_{out}$  are the perturbation discharge and the discharge curve measured at the outlet 8.7 m from the entrance,  $h_{1.0}$  and  $h_{5.5}$  are the depth of flow measured at 1.0m and 5.5m from the entrance, respectively. The wave also induced additional waves as it grew up

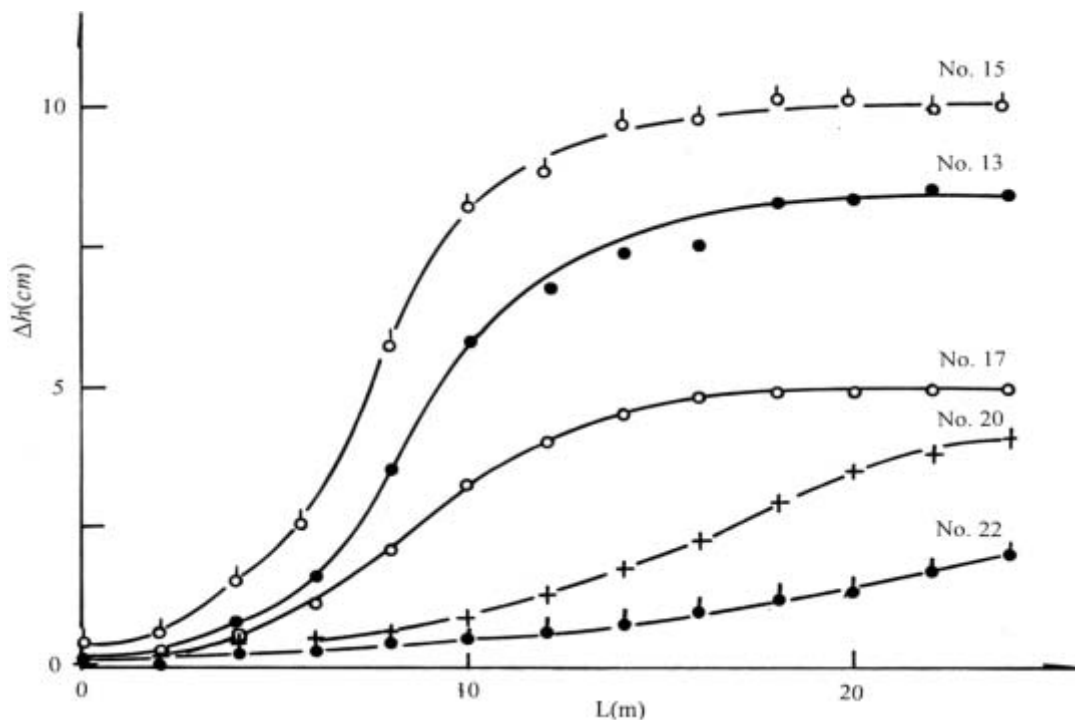


Fig. 7. Growth of the perturbation wave.

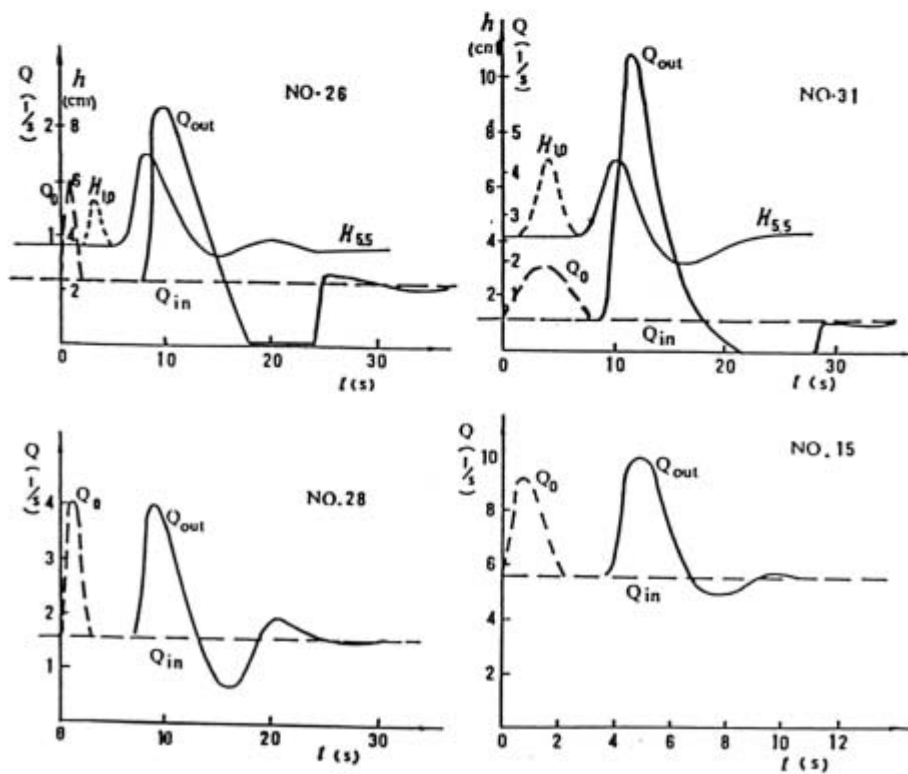
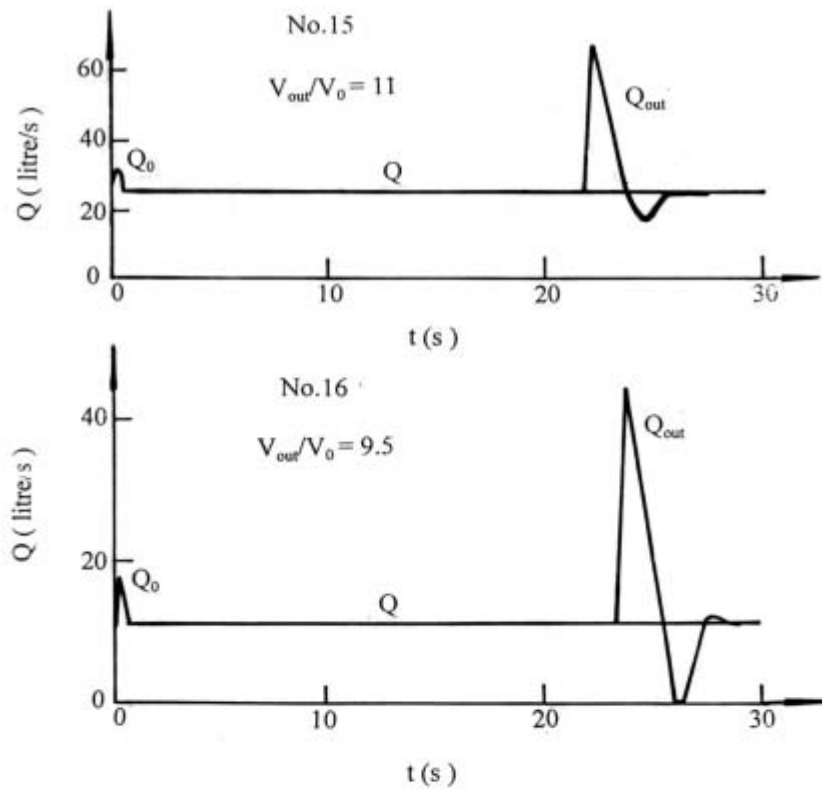


Fig. 8. (a) Discharge of perturbation wave at the entrance and the downstream end of the flume (26 m long, 60cm wide); (b) Discharge of perturbation waves at the entrance and the downstream end of a flume (8.7 m long , 10 cm wide).

and propagated down the channel, as shown in Fig. 8b. Lava flow is also non-Newtonian with large yield stress. Because its viscosity or rigidity coefficient is extremely high and  $S_{vis}$  is much larger than  $S_y$ , therefore, the lava flow is usually stable (Johnson, 1970).

In hyperconcentrated flow in rivers, a perturbation wave could result from such causes as inflow from a tributary, a sharp variation in cross section, a variation of flood discharge, or a change in sediment concentration. The original perturbation wave could

develop into a larger wave or even into 'river clogging' because the hyperconcentrated flow was usually non-Newtonian. A hyperconcentrated flow of volume concentration  $C_v=0.35$  (941 kg/m<sup>3</sup>) occurred in 1975 and the flow was non-Newtonian. The flood wave grew as it travelled from the Xiaolangdi Hydrological Station to the Huayuankou Station (about 100 km down from Xiaolangdi). The flood peaks grew higher and the trough became deeper. The yield stress is smaller than clay concentration because the flow carries a lot of cohesionless material. The parameter  $\tau_B/2\gamma_m h$  is estimated at  $10^{-5}$ , therefore, the wave height growth can be estimated at 0.5 m by travelling the 100-km distance, which coincidentally agree with the measured value.

Qian Y. et al. (1980) investigated hyperconcentrated flow and reported that if the concentration was high and the flow became laminar, the stage and velocity of the flow fluctuated and a stagnant layer near the bed appeared where the fluid stopped flowing. The flow in the entire channel became intermittent as the stagnant layer grew up to the surface. This can also be interpreted by the mechanism given in the paper. The increase in discharge of the debris flow wave along its course in the Little Almakingka River shown in Fig. 2. shares the same mechanism.

### 3.4 Development of Roll Waves

If the clay concentration and the slope are high, the flow depth is small, the flow is so unstable that it may develop into a series of roll waves at constant incoming discharge, even no perturbation wave is introduced. Generally speaking, a slight fluctuation in velocity occurred, then some ripples appeared of the surface. The ripples grew into waves as they propagated downstream, and more other ripples formed at the same time. Sometimes the waves grew so large that their maximum discharges were more than double the incoming one, and the residual mud stopped moving after the waves passed. The roll waves stopped growing when they reached a certain amplitude  $H$ . The law of growing is the same as those shown in Fig. 6. and given in Eq.(19) and (33). The limiting amplitude appeared to be directly related to the depth and the clay concentration. A fully developed wave had the form shown in Fig. 9, in which the streamlines of the flow are seen by a viewer moving with the wave. The wave always propagated

more rapidly than the flow between waves. A part of the clay suspension moved upward like a fountain under the extrusion of the wave as it was caught by a wave. Then it divided into two parts, one part flowed forward at a speed  $2u_w$  ( $u_w$  is the speed of the wave) and formed a rolling front and the other part flowed at a speed less than  $u_w$  and gradually lags behind the wave.

Table 3 presents the main results of the experiments.  $Q_0$  is the discharge at the entrance and maintained constant during the experiment,  $h_0$  the flow depth measured at 2 m from the entrance where the flow was stable and no wave appeared,  $Fr$  the Froude number defined by the average velocity and the depth in the section without wave,  $F$  and  $H$  are the frequency and height of waves measured at the downstream end of the flume. In most of the experiments, ripples appeared in the section 3-9 m from the entrance and developed into waves in the section 5-14 m and stopped growing and maintained constant thereafter. The speed of the wave propagation  $u_w$  was measured in the downstream section where the speed maintained constant, which was much larger than the flow velocity in the upstream section without wave. The growth rate per distance  $\Delta h/L$  was measured in the section of wave growth, which was smaller than the dimensionless number  $S_y/2$  representing the theoretical growth rate of wave. The growth rate is related to  $S_y/2$  in Fig. 6. showing the same law as those of the perturbation-induced wave. The frequency and the amplitude of the waves in the downstream section were relatively stable. Although the flow was wavy and in unstable state but velocity measurement showed that the flows were laminar.

Table 3 Experimental results of roll waves

No.	$C_v$ (%)	$J$ (%)	$Q_0$ (l/s)	$h$ (m)	$u_w$ (m/s)	$Fr$	$S_y/2$	$\Delta h/L$	$F$ (1/s)	$H$ (cm)
25	19	4.0	16	0.070	1.03	0.458	0.019	0.009	0.06	5.7
26	19	6.0	11	0.048	1.13	0.554	0.028	0.015	0.07	4.8
27	19	8.0	10	0.038	1.04	0.720	0.035	0.016	0.08	4.3
28	15.8	8.0	5	0.021	1.04	0.882	0.033	0.019	0.40	3.2
29	15.8	6.0	5	0.025	1.14	0.687	0.028	0.017	0.30	3.4
30	15.8	4.0	10	0.038	0.94	0.721	0.018	0.011	0.32	3.4
31	11.3	2.0	7	0.023	1.55	1.073	0.009	0.003	0.86	3.0
32	11.3	4.0	10	0.015	1.81	2.893	0.014	0.004	1.02	2.1

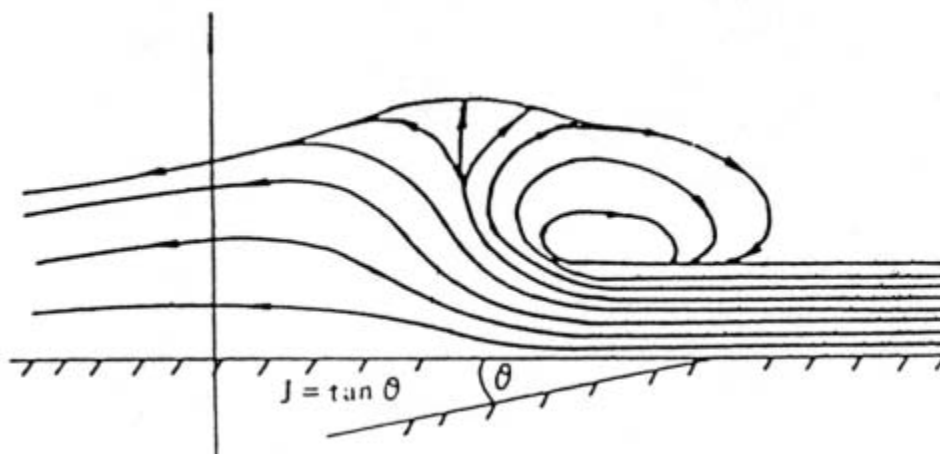


Fig. 9. Profiles of a roll wave.

Comparing the dimensionless number  $S_y/2$  in Table 3 and 2 suggests that the roll waves develop at much larger value of  $S_y/2$ , which represents the instability of the flow. The Froude number is not the essential factor because the flow with small Froude number ( $Fr < 0.5$ ) developed into intermittent flow. This is different from the film flow of water.

The frequency is the number of waves that passed a certain section per unit time. It equals zero for the section near the entrance (stable flow). The frequency increased in the downstream direction, from a point ripples appeared, until reached a certain value,

and then reduced slightly. Some distance was needed for small ripples to develop into waves so that more and more waves came into being downstream from the point; also larger waves propagated faster than smaller waves so that they could catch up with the smaller waves and combined them into still larger waves, resulting in slight reduction in the frequency before it became stable in the last section.

Fig. 10. shows the hydrographs of the discharge and depth in the entrance section,  $Q_0$  and  $h_0$ , and discharge and depth at the downstream end of the flume,  $Q_{out}$  and  $h_{out}$  for the experiment No.25

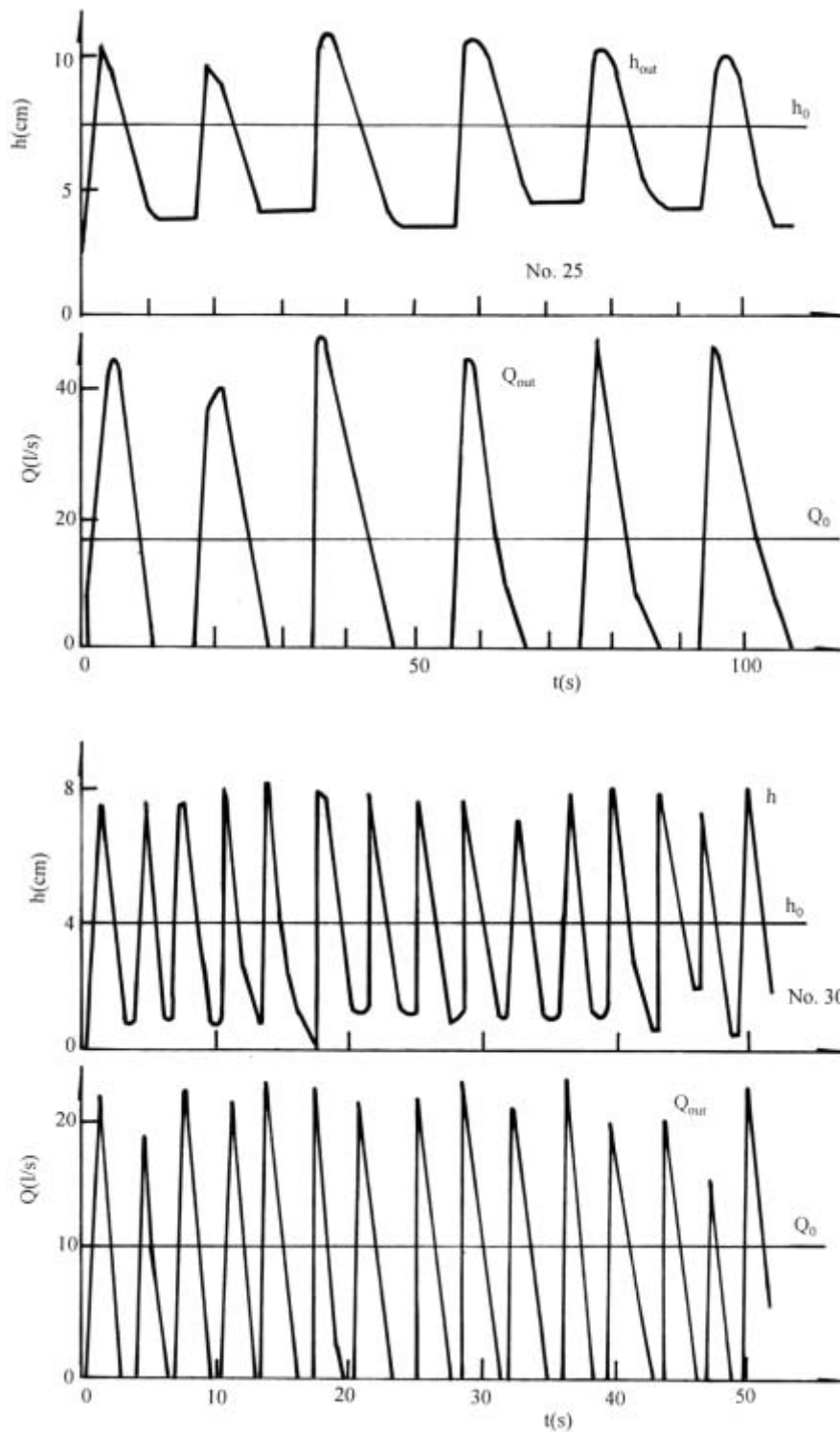


Fig. 10. Development of roll waves ( $h_{out}$  and  $Q_{out}$ ) from stable flow ( $h_0$  and  $Q_0$ ) for the experiments No. 25 and No. 30.

and No.30. It shows that the mudflow at the outlet of the flume fluctuated and even developed into intermittent flows, although the incoming discharge remained constant. The higher the yield stress (concentration), the longer the time interval between the waves appeared to be.

The intermittent flow in Fig. 10. is similar to viscous debris flow. In each case, the slope is large and the depth of the flow is small. Viscous debris flow often develops into roll waves, e.g. debris flow waves occurred in the Jiangjia Gully, Yunnan Province, South China (Kang, 1985). The bed slope of the Jiangjia Gully is 5-10%, and the average flow depth is usually 10-60 cm as viscous debris flow takes place. The matrix of the debris flow has a high yield stress, 100-1000 Pa. The flow developed from a continuous turbulent flow into an intermittent laminar flow and many waves developed as the concentration of solid material rose from  $C_v=0.1$  to  $C_v=0.6$ . The dimensionless number  $S_y/2$  increased from 0 to 0.05, then roll wave developed from continuous flow. Each wave lasted 10-30 seconds, and the time interval between the waves was about 20-100 seconds.

#### 4. Conclusions

Non-Newtonian laminar flow exhibits free surface instability, such as the river clogging in the hyperconcentrated flows, intermittent viscous debris flows and fluctuation in mudflows. Theoretical analysis from the equation of motion incorporating the non-Newtonian nature of the fluid demonstrated that the free surface instability is essentially caused by the yield stress. Two dimensionless numbers,  $S_y$  and  $S_{vis}$ , representing the effects of yield stress and viscosity are calculated and compared for various flows. The free surface is unstable and roll waves may develop even at constant incoming flow rate if  $S_y$  is much larger than  $S_{vis}$  and is stable if  $S_y$  is smaller than  $S_{vis}$ . Experiments show that river clogging occurs if the driving shear stress is nearly equal to the yield stress, a perturbation wave may grow up in non-Newtonian laminar flow if  $S_y$  is large, and a series of roll waves may develop if  $S_y$  is even larger. The experimental results agree well with the theoretical formula showing exponential law of growth of wave height. The growth rate of wave height depends essentially on the parameter  $S_y$ . The larger is the parameter  $S_y$ , the higher is the growth rate and the higher are the waves.

#### Acknowledgement

The study is supported by the National Natural Science Foundation and the Ministry of Water Resources of China (No.59890200).

#### References

CHEN, C.L., 1995, Free surface stability criterion as affected by velocity distribution, *Journal of Hydraulic Engineering, ASCE*, Vol.121, No.2, pp.736-743.  
 DUESHENOV, E.A. and A.C. JACKWETZ, 1979, On the variation of debris flow discharge along its course, *Selection of Translated Papers, Institute of Railway Engineering* (in Chinese).

ENGELUND, F. and WAN ZHAOHUI, 1984, Instability of hyperconcentrated flow, *J of Hydraulic Engineering*, Vol. 110, No.3, pp. 219-233.  
 GUO ZHIGANG, ZHOU BIN, LING LAIWEN and LI DEGONG, 1985, The hyperconcentrated flow and its related problems in operation at Hengshan Reservoir, *Proc. Intern. Workshop on Flow at Hyperconcentrations of Sediment, IRTCES*, Sep. Beijing, China.  
 JOHNSON, A., 1970, *Physical Process in Geology*, Freeman Cooper & Company, California.  
 KANG ZHICHENG, 1985, Characteristics of the flow patterns of debris flow at Jiangjia Gully in Yunnan, *Memoirs of Lanzhou Institute of Glaciology and Cryopedilogy*, No.4 (in Chinese).  
 PIERSON T.C., 1986, Flow behavior of channelized debris flows, Mount St. Helens, Washington, in *Hillslope Processes*, eds by Abrahams, Allen & Unwin Publishers, pp.269-296.  
 QIAN NING and WAN ZHAOHUI, 1983, *Dynamics of Sediment Movement*, Chinese Science Press (in Chinese).  
 QIAN YIYING et al., 1980, Basic characteristics of flow with hyperconcentration of sediment, *Proc. Intern. Symp. on River Sedimentation*, Guahua Press, Mar. China.  
 SAWADA T. and SUWA H., 1994, Debris flow observed in the period during 1991-1993, *Research Report of Grant-in-Aid for International Scientific Research Program No.03044085 of the Ministry of Education, Science, Sports and Culture of Japan*, pp.42-55.  
 SUWA H. and SUMARYONO A., 1996, Sediment discharge by-storm runoff from a creek on Merapi volcano, *J. of Japan Soc. Erosion Control Engineering*, Vol.48, Special Issue, pp.117-128.  
 TRITTON, D.J., 1977, *Physical Fluid Dynamics*, Van Nostrand Reinhold Company, pp.201-213.  
 VEDERNIKOV, V.V., 1945, Conditions at the front of a translation wave disturbing a steady motion of a real fluid, *Comptes Rendus (Doklady) de l'Academie des Sciences de l'URSS*, 48 (4), pp.239-242.  
 WAN ZHAOHUI and WANG ZHAO-YIN, 1994, *Hyperconcentrated Flow*, Balkema Publishers  
 WAN ZHAOHUI, QIAN YIYIN, YANG WENHAI, and ZHAO WENLIN, 1979, Laboratory study on hyperconcentrated flow, *People's Yellow River*, pp.53-65 (in Chinese).  
 WANG ZHAOYIN, LIN BINGNAN and ZHANG XINYU, 1990, Instability of non-newtonian fluid flow, *Mechanica Sinica*, No. 3, pp.266-275 (in Chinese).  
 WANG ZHAOYIN, 1992, Model test of non-newtonian fluid flow, *Proc. 5th Intern. Symp. on River Sedimentation, IWK and IRTCES, Karlsruhe, F.R. Germany*.  
 WANG ZHAOYIN, LARSEN PETER and XIANG WEI, 1994, Rheological properties of sediment suspensions and their implications, *Journal of Hydraulic Research*, Vol.32, No.4, pp.495-516.  
 WANG, ZHAOYIN, REN, YUMIN and WANG, XINKUI, 1995, Total pressure velocimeter for the measurement of turbulence in sediment-laden flows, *Proceedings of 2nd International Conference on Hydro-Science and Engineering, CHES and IRTCES, March, Beijing, China*.